A Large, Voltage-Dependent Channel, Isolated from Mitochondria by Water-Free Chloroform Extraction

Evgeny Pavlov,* Eleonora Zakharian,† Christopher Bladen,* Catherine T. M. Diao,* Chelsey Grimbly,* Rosetta N. Reusch,† and Robert J. French*

*Department of Physiology and Biophysics, University of Calgary, Alberta, Canada; and †Department of Microbiology and Molecular Genetics, Michigan State University, East Lansing, Michigan, USA

ABSTRACT We examined ion channels derived from a chloroform extract of isolated, dehydrated rat liver mitochondria. The extraction method was previously used to isolate a channel-forming complex containing poly-3-hydroxybutyrate and calcium polyphosphate from *Escherichia coli*. This complex is also present in eukaryotic membranes, and is located primarily in mitochondria. Reconstituted channels showed multiple subconductance levels and were voltage-dependent, showing an increased probability of higher conductance states at voltages near zero. In symmetric 150 mM KCl, the maximal conductance of the channel ranged from 350 pS to 750 pS. For voltages $>\pm 60$ mV, conductance fluctuated in the range of $\sim$50–$\sim$200 pS. In the presence of a 1:3 gradient of KCl, at pH = 7.4, selectivity periodically switched between different states ranging from weakly anion-selective ($V_{rev} \sim -15$ mV) to ideally cation-selective ($V_{rev} \sim +29$ mV), without a significant change in its conductance. Overall, the diverse, but highly reproducible, channel activity most closely resembled the behavior of the permeability transition pore channel seen in patch-clamp experiments on native mitoplasts. We suggest that the isolated complex may represent the ion-conducting module from the permeability transition pore.

INTRODUCTION

It is well established that mitochondria possess many different ion-transporting systems, which play central roles not only in mitochondrial function but also in regulation of fundamental processes ranging from cellular protection during ischemia/reperfusion (Garlid and Paucek, 2001) to apoptosis (Mattson and Kroemer, 2003; Danial and Korsmeyer, 2004). Although mitochondrial ion transport systems have been described in great detail in vivo, by using single-channel patch clamp of isolated mitochondria, and by other methods, much controversy remains about molecular mechanisms (Zoratti and Szabo, 1995; Carafoli, 2003; Green and Kroemer, 2004). A most interesting and important task is to determine the molecular composition of the mitochondrial permeability transition pore (PTP). The significance of this problem became evident in recent years, after it was demonstrated that opening of the PTP plays a central role in apoptosis (Halestrap and Brennerb, 2003). Although several hypotheses are being considered at this time, there is still no clear resolution of this issue (Green and Kroemer, 2004).

On the other hand, a great deal of progress has been made lately in identifying relations between bacterial and eukaryotic ion channels. A number of bacterial and eukaryotic plasma membrane channels, which possess conserved regions in their DNA sequences, demonstrate similar electrophysiological properties, such as ion selectivity and voltage-dependent gating (Doyle et al., 1998; Durell and Guy, 2001; Accardi and Miller, 2004). It is also well-established that, in evolutionary terms, mitochondria originate from bacteria (Dyall et al., 2004). This led us to consider the possibility that not only do mitochondria from eukaryotic cells contain channels homologous to bacterial ones, but that mitochondria might have ion-transporting systems that are more closely related to bacterial ion-transporting systems than to the ion channels of the eukaryotic plasma membrane.

With this idea in mind, we tried to determine which bacterial channels might most likely be present in mitochondria. It is known that *Escherichia coli* and some other bacteria contain a channel with a distinctive chemical structure. Extensive data suggest that this channel consists of a poly-R-3-hydroxybutyrate/polyphosphate/calcium (PHB/polyP/Ca^{2+}) complex (Reusch et al., 1995). Although certain properties of this channel are believed to be regulated by noncovalently associated protein (Das et al., 2002), it was shown by total chemical synthesis that these three components are sufficient for formation of the channel (Das et al., 1997). It was also shown that the stability of this complex is extremely sensitive to the extraction conditions. Thus far, this is the only nonproteinaceous channel of biological origin known.

Notably, it was demonstrated that a similar chemical complex is also present in eukaryotic organisms, where it is primarily found in mitochondria (Reusch, 1989). Here, we have applied a similar extraction protocol to isolated mitochondria to determine whether we could detect channel-forming activity after reconstitution of the chloroform extract into lipid bilayers. One hypothesis that we considered is that the complex might function as the ion conductance

Submitted November 30, 2004, and accepted for publication January 26, 2005.

Address reprint requests to Robert J. French, Dept. of Physiology and Biophysics, University of Calgary, Calgary, Alberta, Canada T2N 4N1. Tel.: 403-220-6893; Fax: 403-283-8731; E-mail: french@ucalgary.ca.

0006-3495/05/04/2614/12 $2.00

doi: 10.1529/biophysj.104.057281

pathway of the mitochondrial calcium uniporter complex—a possibility very recently proposed by others (Brookes et al., 2004). To our surprise, although the reconstituted channel activity at voltages above ±60 mV resembled the activity of the complex isolated from *E. coli*, at the lower voltages we observed channel activity with distinctive properties that were similar to those of the permeability transition pore.

MATERIALS AND METHODS

Isolation of mitochondria

Mitochondria were isolated from the liver of Sprague-Dawley rats (200–250 g) by differential centrifugation. Liver from four rats was homogenized using Teflon-glass homogenizer and resuspended in 150 ml of the isolation buffer, containing 70 mM sucrose, 230 mM mannitol, 5 mM Hepes-KOH, pH = 7.4. Unbroken cells were centrifuged at 600 × *g* for 15 min. The supernatant was collected and spun at 8500 × *g* for 20 min. The resulting pellet was resuspended in 10 ml of the isolation buffer. In some experiments, isolated mitochondria were resuspended in 100 ml of isolation buffer to which 5 mM glutamic acid, 1 mM KH_2PO_4, 10 mM $CaCl_2$, pH = 7.4 were added and incubated at room temperature for 10 min, and subsequently collected by centrifugation and resuspended in 10 ml of isolation buffer. This calcium treatment led to increased frequency of observations of channel activity (see Results). The mitochondrial pellet was collected after the final spin at 8500 × *g* for 20 min.

Extraction of channels from the mitochondria

Isolated mitochondria were dehydrated by sequential washes with methanol, methanol-acetone, and acetone, as follows. The mitochondrial pellet was resuspended in methanol at a concentration of ~10 mg protein/ml (total volume of methanol 30 ml), incubated for 10 min, and then spun down at 3200 × *g* for 15 min (twice). The procedure was repeated with 30 ml of methanol/acetone, 1:1 (twice), and then with acetone (twice). Traces of acetone were removed from the final pellet with a stream of dry nitrogen. The yield in the final pellet was ~150 mg dry weight from a mitochondrial fraction containing 300 mg protein. The dried pellet could be stored for up ~1 month without loss of channel activity. Typically, chloroform extraction was done by incubating ~50 mg of dry pellet in 5 ml chloroform at 4°C for 24–48 hr, in Teflon tubes (Nalgene). Importantly, all solvents used during the process of dehydration and extraction were ice-cold, and were pretreated with molecular sieve beads, 8—12 mesh (No. 208604, Sigma-Aldrich, St. Louis, MO), to eliminate all traces of water. All procedures were performed on ice.

Incorporation of the chloroform extract into black lipid bilayers and current recordings

Before channel incorporation, the chloroform suspension was filtered a 0.2 μm PTFE filter (Acrodisc Syringe Filter, PALL Life Sciences, East Hills, NY) using a Teflon syringe. The filtered extract was used within 3–4 h. For bilayer formation, the filtered chloroform extract from 0.1–5 mg of dry mitochondrial pellet was dispersed in 50 μl of a decane-lipid mixture (10 mg/ml, POPE, Avanti Polar Lipids, Alabaster, AL). Bilayers were formed by painting with the mixture containing chloroform extract, decane, and lipid on an aperture of 100 or 200 μm diameter in the wall of a Teflon cup (Warner Instruments, Hamden, CT). Similar channel activity was observed with each of two procedures for making the mixture of decane, lipid, and mitochondrial extract. Either the filtered mitochondrial chloroform extract was mixed with chloroform-lipid stock solution, dried, and the residue taken up in the appropriate amount of decane, or small volumes of the mitochondrial chloroform extract (less than or equal to the volume of decane) were added directly to a dispersion of lipid (10 mg/ml) in decane.

The sign of the voltage is that of the opposite chamber from which the lipid/chloroform mixture was painted, and cannot be rigorously associated with a particular channel orientation. Experiments were done using silver-chloride electrodes without salt bridges. Net junction potentials were set to zero before bilayer formation and tested again after membrane disruption at the end of each experiment. In all experiments shown, junction potential drift was <2 mV and was not considered significant. Uncompensated junction potentials for 150 mM–50 mM gradient of KCl were estimated to be 0.5 mV using JPCalc (Barry, 1994), supplied with pClamp software. All recordings were done at room temperature (20–22°C). In experiments to study selectivity by measuring reversal potential shifts, the concentration gradient was created and the junction potential offset was compensated before membrane painting. Solutions were not changed during an experiment, so absolute values of half-cell potentials at the Ag/AgCl surfaces had no effect on measurements of shifts in reversal potential. Unless otherwise stated, records were filtered to 100 Hz (–3dB, low pass, 4-pole Bessel filter) before digitizing at 2 kHz. Recording solutions contained: 200 mM $CaCl_2$, 5 mM $MgCl_2$, 5 mM Tris-Hepes; 150 mM KCl, 20 mM Tris-Hepes or 100 mM NaCl, 20 mM Tris-Hepes. All solutions were adjusted to pH 7.4, unless otherwise stated. Data were collected with an Axopatch-1B amplifier, filtered at 100 Hz and digitally recorded to a PC, using pClamp 9.0 software (Axon Instruments, Foster City, CA).

Single-channel properties reported in this article are representative from ~100 single-channel experiments observed after reconstitution of chloroform extracts from 15 separate rat liver mitochondrial isolations.

Data analyses

Single-channel analysis was done using Clampfit 9.0 software. Figures of current traces were prepared in Origin 7.0. Linear fits of I/V plots were done using SigmaPlot 8.0.

Protein and Polyphosphate assays

For visualizing of proteins, 10% SDS-PAGE gels were stained Bio-Rad using a SYPRO Ruby staining kit (No. 170-3138; Bio-Rad, Hercules, CA). Proteins were visualized using a ProXPRESS PerkinElmer (Wellesley, MA) multiwave scanner. Polyphosphates were visualized by toluidine blue staining of 15% PAGE gels (acrylamide/bis, 19:1). The identity of the polyphosphates was further confirmed by observing their digestion by exopolyphosphataseX (courtesy of A. Kornberg, Stanford University, Stanford, CA) (Wurst and Kornberg, 1994), control sample was treated with proteinase K (in 10 mM Tris-HCl, pH 7.5) (Boehringer Mannheim GmbH, Mannheim, Germany). For immunoblotting, the proteins were stained for ATP synthase subunit *c* detection using a polyclonal antiserum (a kind gift of Dr. D. N. Palmer, Lincoln University, Christchurch, New Zealand) (Palmer et al., 1995).

Polyhydroxybutyrate assay

PHB was determined by a chemical assay using a variation of the method of Karr et al. (1983) as previously described. The dry sample was hydrolyzed by heating in 0.5 ml concentrated sulfuric acid at 92°C for 20 min. The sample was cooled on ice, diluted by addition of 1 ml. saturated sodium sulfate, and extracted three times with 2 ml methylene chloride. The methylene chloride extracts were transferred to a vial and mixed with 100 μl of 5 N NaOH to convert the volatile crotonic acid to the less volatile sodium salt. Methylene chloride was then removed by evaporation with dry nitrogen and the sample was stored at −20°C.

Just before chromatography, the sample was re-acidified by addition of 100 μl of 5 N H_2SO_4. Crotonic acid was separated by high-performance liquid chromatography on a Bio-Rad Ion Exclusion column (HPX-87H)

using 0.014 N H_2SO_4 as eluent, and quantified by comparison of the peak area with that of crotonic acid standards.

The chain length of PHB was examined by nonaqueous size-exclusion chromatography on a Shodex GPC K803 column using dry chloroform as eluent. The elution time of the mitochondrial PHB was the same as that of the PHB extracted from *E. coli* membranes, whose size has been determined by electrospray mass spectroscopy as 12.2 kDa (Reusch, 2001).

RESULTS

Channel-forming activity of chloroform extracts from isolated mitochondria

We found that channel-forming activity of chloroform extract strongly depended on the extraction conditions. Channel activity was not observed when mitochondria were not dried and delipidated before chloroform extraction, or when extraction was not performed in Teflon tubes using anhydrous chloroform. A noticeable increase in frequency of channel detection was observed when intact mitochondria were incubated with 10 mM calcium before methanol-acetone treatment and chloroform extraction. Without this calcium pretreatment, activity was observed in 1–2% of the total number of painted bilayers compared with up to 20% after pretreatment. In Figs. 1–6, and in the following sections, we illustrate the complex, but consistently observed, characteristics of the channels seen in recordings from planar lipid bilayers.

Single-channel conductance at low voltages

Typical channel activity, observed at lower voltages (from −30 to +30 mV), is presented in Fig. 1. At this voltage, the single-channel currents mostly fluctuated near the highest conductance state, with brief closures to lower conductance substates. In most experiments, when the channel was near its maximum conductance, small, continuous conductance fluctuations were observed (shown as expanded segments of the recording in Fig. 1 *A*). These conductance fluctuations were usually observed when the channel was near its highest conductance state but not at lower conductance substates. Similar behavior was observed in the presence of three different cations. The current-voltage relationship of the fully open channel was well fit by a straight line (Fig. 1 *B*). Typical single-channel conductance was ~550 pS in 150 mM KCl, ~450 pS in 100 mM NaCl, and 1.2 nS in 200 mM $CaCl_2$. However, in different experiments, channel size varied within the range of 350 pS up to ~750 pS (with symmetric 150 mM KCl), without qualitative differences in channel gating kinetics. A histogram showing the distribution of the detection frequency of channels against conductance is presented in Fig. 1 *C* (based on the analysis of 78 single-channel recordings in the presence of 150 mM KCl). The mean conductance and standard deviation obtained from Gaussian fit of the histogram were 540 ± 120 pS. With this number of experiments, we were unable to determine whether the data reflect a true Gaussian distribution, or if certain discrete, preferred conductance levels exist within this range.

Voltage dependence of the channel activity

At higher voltages, the channel tended to switch to lower conductance states. We observed at least six different subconductance levels. Fig. 2 *A* illustrates several commonly observed fluctuation patterns and conductance substates. All traces shown in Fig. 2 *A* were observed in the same experiment. In all stable recordings showing the typical high conductance at the lower voltages (Fig. 1 *A*), a step increase in voltage was followed by a transition to a stable, lower conductance range, with return to maximal conductance levels when the voltage decreased. In Fig. 2 *A* (*two upper traces*), the channel reopened to its highest conductance state after membrane potential was decreased to 20 mV from 40 mV. Fig. 2 *A* (*lowest trace*) represents a rare event (observed in five different channels), in which a voltage step to a higher potential induced almost complete closure of the channel interrupted by spikes to a higher conductance state. Fig. 2 *B* presents an all-points histograms of the single-channel conductance. These histograms were taken from current traces of at least 120 s in duration, immediately (~1 s) after application of a voltage step. Before the voltage step, the channel was in the maximal conductance range (Fig. 1 *A*). The sampled period spans nonstationary fluctuations, shortly after the pulse application, as well as near stationary behavior in the later part of the sampled interval. As can be seen, with an increase in voltage, the channel preferentially stayed in lower conductance states. In general, the time required for the channel to reach a steady distribution of subconductances depended on the applied voltage, and was shorter for higher voltages. Although multiple conductance substates were observed, it can be seen that, in general, channel conductance decreased with voltage.

In Fig. 3, we illustrate some different, representative patterns of single-channel fluctuation observed in the low conductance range. Application of the voltages >~50 mV, of either negative or positive polarity, induced channel transitions to a pseudostationary lower conductance range. Representative current recordings from channels fluctuating in this range are shown in Fig. 3. For all presented recordings, at the beginning of the experiment and at low voltage, each channel was in its maximal conductance range, with characteristic fluctuations in and out of their peak conductance state, as shown in Fig. 1 *A*. In Fig. 3, *A* and *B*, the channels show similar, predominant conductances (~100 pS) despite different ionic conditions (symmetric 200 mM $CaCl_2$ and symmetric 200 mM KCl, respectively). The channel in Fig. 3 *C* showed relatively fast, voltage-dependent fluctuations in the low conductance range. Note that, for Fig. 3 *C*, values of conductance were determined from the slopes of the I/V plots due to the presence of the salt

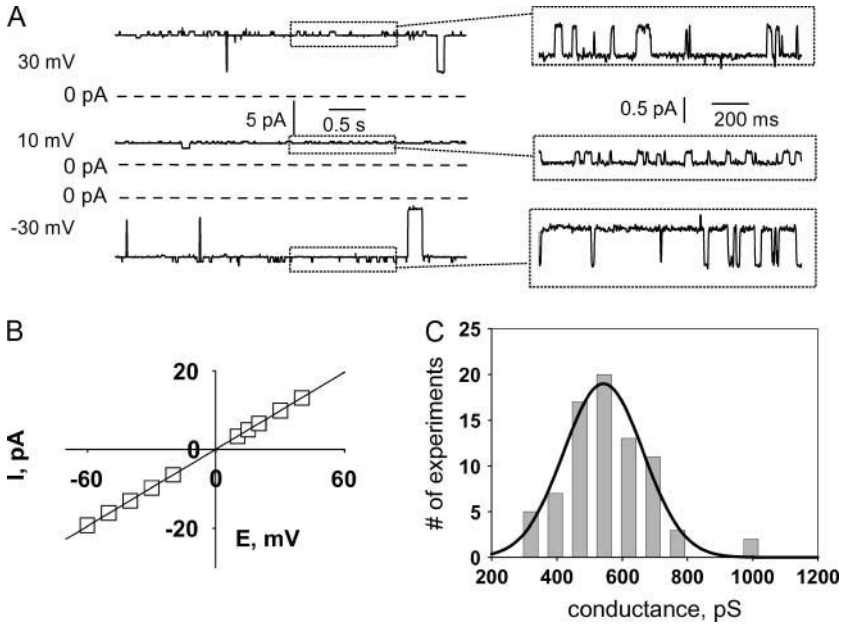

FIGURE 1 Representative single-channel activity recorded from a lipid bilayer membrane after incorporation of material from the mitochondrial chloroform extract. (*A*) Recording solutions contained 150 mM KCl, 20 mM Tris-Hepes, pH = 7.4. Expanded sections of the records (*boxed*) show the highly characteristic, smaller conductance fluctuations from the maximal conductance level. (*B*) I/V relationship of the maximal conductance state of the channel. (*C*) Histogram of the distribution of the detection frequency plotted against maximal conductance, based on the analysis of 78 single-channel recordings in the presence of 150 mM KCl. Mean conductance (± SD) obtained from a Gaussian fit of the histogram was 540 ± 120 pS. Note that in some experiments included into the histogram, 1 mM of $CaCl_2$ was present in the recording solutions. Such experiments were included in the analysis after it was established that addition of 1 mM $CaCl_2$ did not cause any detectable change of the conductance.

gradient between the two sides of the membrane. This determination gave conductance values of ~200 pS for the S1 substate and ~100 pS for the S2 substate. Thus, traces shown in Fig. 3 demonstrate two predominant kinetic modes observed for the lower conductance state: slow and voltage-independent (Fig. 3, *A* and *B*) and fast with decreased probability of the higher S1 conductance state at higher voltages (Fig. 3 *C*). Interestingly, although the initial channel transition to the lower conductance state shown in Fig. 3 *C* required application of a high voltage (see above), the channel stayed in the lower conductance range after moderate potential decreases. Notably, the kinetic behavior was apparently not determined by the ionic conditions, but rather, seemed to reflect the properties of the channel.

Multiple selectivity states of the channel

Cation-anion selectivity of the channel was studied in the presence of a 1:3 gradient of KCl, at pH = 7.4. The compartment connected to the reference electrode contained 150 mM of KCl and the compartment connected to the command electrode contained 50 mM KCl. Selectivity of a certain channel conductance state was determined by measuring the reversal potential. The reversal potential was estimated by plotting the single-channel current as a function of voltage for each distinct conductance-selectivity state and linearly extrapolating these I/V relationships to the zero current. Fig. 4 shows an example of such an experiment. In the current trace shown in Fig.4 *A*, two different selectivity states can be recognized. In this case, a transition between states occurred spontaneously at −5 mV (indicated by an *arrow*). Current-voltage relations for two conductance states are presented in Fig. 4 *B*. As can be seen from the analysis, the channel initially appeared to be cation-selective with an estimated $V_{rev} = +16$ mV. It then spontaneously switched to an anion-selective state with an estimated $V_{rev} = -10$mV, as shown by the jump of the current trace across zero (see *arrow* in Fig. 4 *A*), at constant voltage.

In addition to the observed selectivity switch, other transitions from one conductance/selectivity state to another were observed without voltage change, sometimes reverting to the original state within a few seconds. Fig. 4 *C* demonstrates such an event, in which, at −5 mV, the channel switched from its anion-selective state to a cation-selective and back. Note that the kinetic behavior of the small current fluctuations differed substantially, whereas their conductances were nearly identical. For the anion-selective state, openings to the higher conductance state were 5–10 times shorter than for those in the cation-selective state. Fig. 4, *D* and *E*, shows dwell time histograms of the open state for anionic and cationic selectivity states, respectively.

We also observed several other selectivity states. Fig. 5 represents an overview of an analysis of single-channel selectivity obtained from the experiment shown on Fig. 4, based on apparent changes in reversal potential, in different small periods within a continuous recording. Although extrapolation of I/V relations to estimate reversal potentials can produce misleading results, two factors suggest that this procedure is reasonable in this particular case. First, I/V relations for cases where a clear kinetic pattern of fluctuations is maintained over a range of voltages are essentially linear (Fig. 1 *C*). Second, the threefold concentration gradient chosen is large enough to reveal unambiguous shifts in reversal potential if selectivity changes, but is small enough to minimize errors in short-range extrapolations to estimate of reversal potential. For example, the Goldman

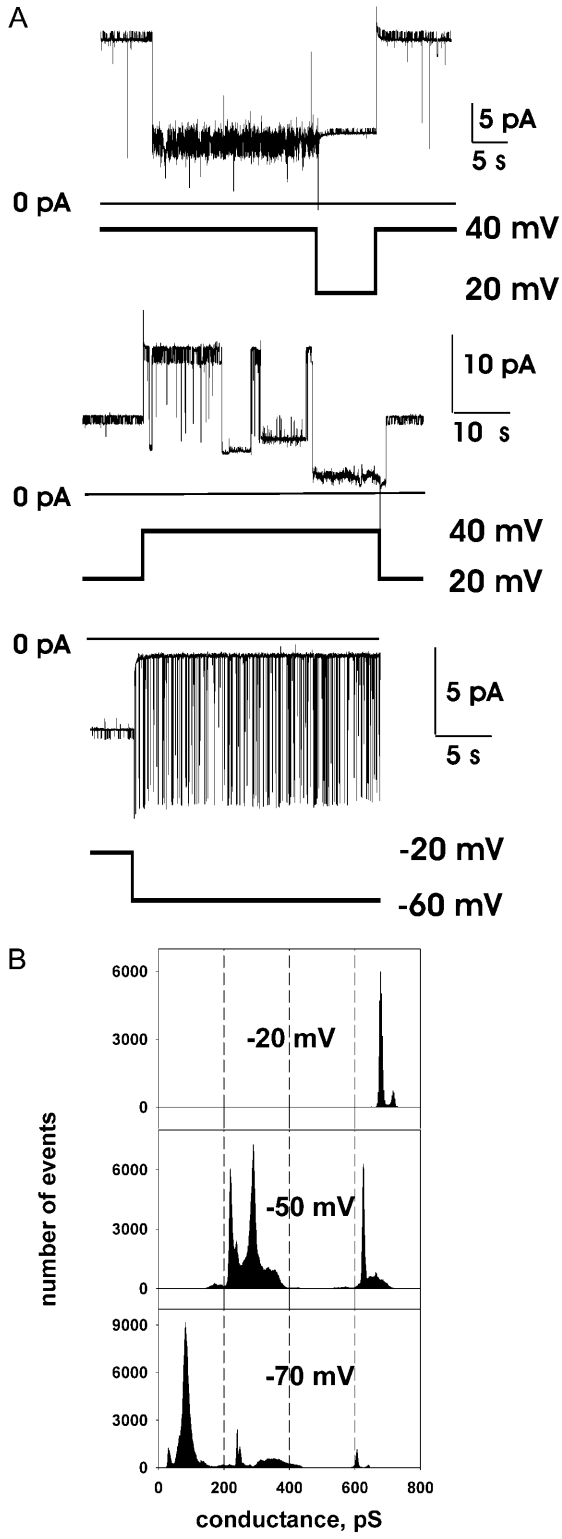

FIGURE 2 Multiple conductance substates and voltage-dependence of single-channel fluctuations. (*A*) Typical channel behavior in response to the step changes in voltage demonstrates the presence of multiple conductance states. Discrete changes in conductance were, in many cases, closely associated with step changes in voltage, e.g., in the upper trace the step from 40 to 20 mV leaves the current amplitude unchanged, reflecting an increase in conductance associated with the downward voltage step. Despite some stochastic variation, in most cases, a step decrease of the voltage transferred the channel back to its maximal conductance state (*two upper traces*). Recording solutions contained 150 mM KCl, 20 mM Tris-Hepes, pH = 7.4. (*B*) All-points histograms of the channel conductance, estimated from Ohm's law (see Fig. 1 *C*) at different voltages. The data were recorded from the experiment shown in panel *A*. Each histogram represents data from at least 120 s of record. The start of the record for each histogram was taken immediately after (~1 s) the voltage step to the value indicated, and the channel was in the fully open state immediately before the pulse. Note that, at larger deviations from zero voltage, the channel mostly resided in lower conductance substates.

current equation predicts a maximal threefold change in slope from large negative to large positive voltages. Due to the very complex behavior and multiple conductance levels of the channel, we were able to identify clearly only a few selectivity states, but we consider it likely that more states exist. In Fig. 5, we limited our selectivity analysis to record segments in which there was a maintained pattern of small fluctuations typical of a particular channel state (e.g., the minor current fluctuations characteristic of the principal state of the channel). The fully open channel can be strongly cation selective with measured $V_{rev} \approx 29$ mV ($E_K = 28$ mV). Interestingly, unlike the switch between cation and anion selectivity, a switch between different cationic selectivity states was not associated with any obvious change in the small current fluctuations. In this example, we estimated from the dwell-time histograms $\tau_{open} = 75$ ms for the more cation selective state ($V_{rev} = +29$ mV, *open triangles*, Fig. 5) and $\tau_{open} = 73$ ms for the less cation-selective state ($V_{rev} = +16$ mV, *open diamonds*, Fig. 5). Also noteworthy is that we were able to identify a lower conductance state, showing cation selectivity, with $V_{rev} = +29$ mV (*open circles*, Fig. 5). This complex behavior presumably reflects multiple conducting conformations of the channel.

Effects of cyclosporin A, lanthanum, pH, and an antibody to ATP synthase subunit C

The observed channel activity was not sensitive to cyclosporin A (1 μM), a potent inhibitor of the mitochondrial permeability transition pore. However, the channel activity was inhibited by 0.5 mM of La^{3+} in a state-dependent manner. When in the maximal conductance state, the channel was unaffected by addition of lanthanum (five experiments), but single-channel current was strongly blocked from a lower conductance substate (10 experiments), and this block was reversed by washout (five experiments, i.e., all experiments in which washout was attempted). This behavior is illustrated in the experiment shown in Fig. 6. At the beginning of the trace, the channel was fully open; then, after it spontaneously switched to its lower conductance substate, 0.5 mM of lanthanum was added, inducing a step decrease in channel conductance. Due to the complicated nature of channel

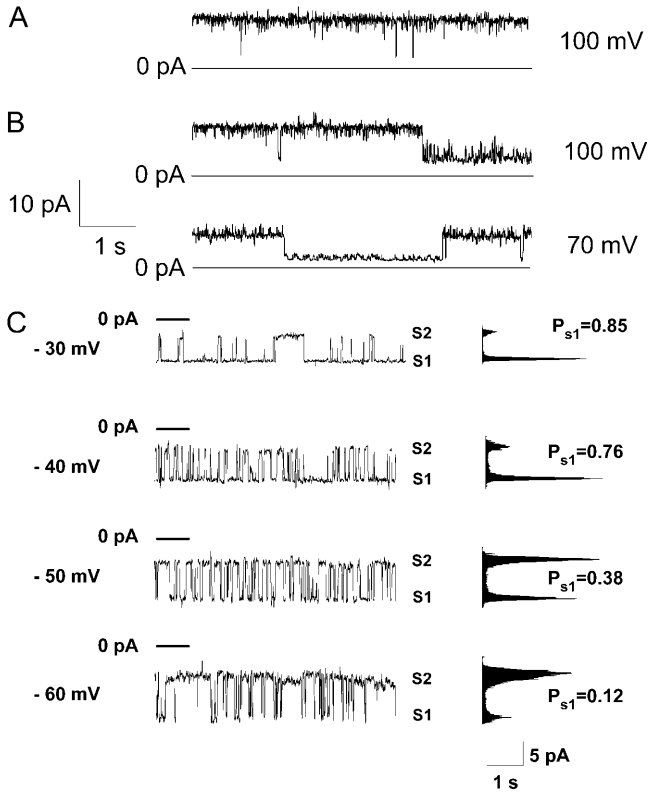

FIGURE 3 Representative single-channel recordings from channels in the lower conductance substates. For all experiments illustrated here, the channels showed stable, higher conductance states at the lower voltages (as in Fig. 1), and a transition to the lower conductance range was induced by stepping the voltage above 50 mV before the segments of recording shown in the figure (as in Fig. 2 *B*). (*A*) Trace recorded in the presence of symmetric 200 mM $CaCl_2$. Maximal conductance shown here, ~100 pS; peak conductance seen at lower voltage, 1.2 nS. (*B*) Traces recorded from a single channel in the presence of symmetric 150 mM KCl. Maximal conductance shown here, ~100 pS; peak conductance seen at lower voltage, 610 pS. (*C*) A different kinetic mode, observed in the low-conductance range, characterized by fast, voltage-dependent gating. P_{S1} represents the probability of the channel being in the substate, S1. Membrane conductance, with the channel in S1, was ~200 pS, and in state S2, ~100 pS, as determined from the slope of the single-channel I/V relationships. The bath compartment connected to the ground electrode contained 65 mM $CaCl_2$, 5 mM $MgCl_2$ and 10 mM NaCl. The opposite chamber contained 1 mM $CaCl_2$, 5 mM $MgCl_2$, and 200 mM NaCl; both solutions were adjusted to pH = 7.4 (10 mM Tris-Hepes).

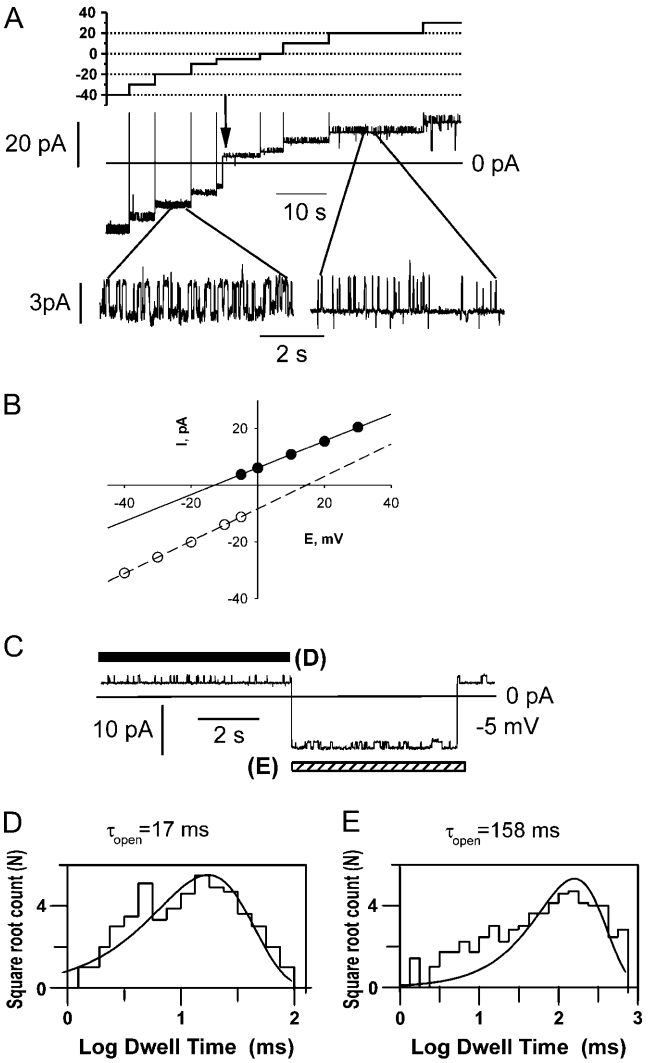

FIGURE 4 Spontaneous selectivity changes by the channel, recorded in presence of a threefold gradient of KCl. The compartment connected to the reference electrode contained 150 mM KCl. The opposite compartment contained 50 mM KCl. All solutions were adjusted to pH = 7.4 (10 mM Hepes-Tris). (*A*) Representative current trace, recorded during a series of progressive voltage steps, used to determine reversal potentials of different selectivity states. (*B*) I/V relationships, obtained by measuring the principal current level at each voltage. Reversal potentials were estimated by extrapolation, to zero current, of the linear fits to the I/V relations, and were −15 mV for the more anion selective state and +15 mV for the more cation selective state. (*C*) An example of reversible, spontaneous transitions between selectivity states, observed at −5 mV, leading to transitions across zero current in the absence of a voltage change. Bars indicate the types of selectivity states that were used for the kinetic analyses shown in panels *D* and *E*. For the actual analysis, longer segments than those illustrated here were used. (*D*) Dwell time histogram, determined at −5 mV, for the higher conductance level in the anion-selective state ($V_{rev} = -15$ mV, $\tau_{open} = 17$ ms, 202 events). (*E*) As in part *D*, but for the cation-selective state ($V_{rev} = 15$ mV, $\tau_{open} = 158$ ms, 203 events).

behavior, we cannot determine conclusively whether the residual conductance represents membrane leak or whether it includes a lower conductance state of the channel. After washout, the channel reopened to the same subconductance state as observed before lanthanum addition and later reopened to the maximal conductance state. Note that in this record, the channel transition back to the substate after washout was associated with a brief voltage step to +20 mV, although such a voltage step was not essential to observe recovery. Lowering the pH to values <6 irreversibly abolished channel activity (seven experiments, data not shown). Channel activity was insensitive to addition of antibodies against subunit C of mitochondrial ATP synthase. These antibodies are known to block the channel formed by subunit C peptide (McGeoch and Guidotti, 1997).

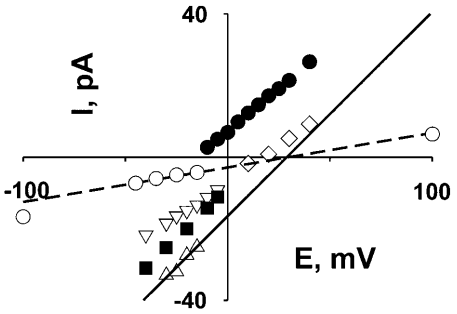

FIGURE 5 Multiple cation conductance and selectivity states. Selectivity of each state was estimated by using the extrapolated reversal potentials. Graph represents I/V plots measured in the presence of 1:3 gradient of KCl (50 mM:150 mM) used for reversal potential determination for each selectivity state. All solutions were adjusted to pH = 7.4 (10 mM Hepes-Tris). Selectivity analysis was limited to the current levels, where typical small current fluctuations were observed, indicating the principal conductance state of the channel. Reversal potential was determined only for relatively stable states, when it was possible to measure the current level at several voltages over a range, with reasonable certainty that the channel did not exit to another state. Recording fragments used for such estimates are similar to ones shown in Fig. 4 *A*. Estimated values for the reversal potentials, and corresponding slope conductances, for the identified selectivity states are the following: anion-selective (●), −15 mV, 470 pS; cation-selective, +15 mV, 560 pS (■); +16 mV, 370 pS (◇); +21 mV, 350 pS (▽); ideally cation-selective, +29 mV, 560 pS (△). Under these experimental conditions, the Nernst potential for potassium equals +28 mV. Ideally, cation-selective states were observed for both maximal conductance (△) and lower-conductance (○) states; the lines are linear fits to the I/V relationships of these two states, as used for determination of reversal potentials.

Chemical composition of the chloroform extract

To determine the chemical composition of the extract, we analyzed its protein composition by using SDS-PAGE electrophoresis using SYPRO Ruby stain, which has a lower protein detection limit of <10 ng. As seen in Fig. 7 *A*, lane 2, a heavy band of low molecular weight peptide was detected

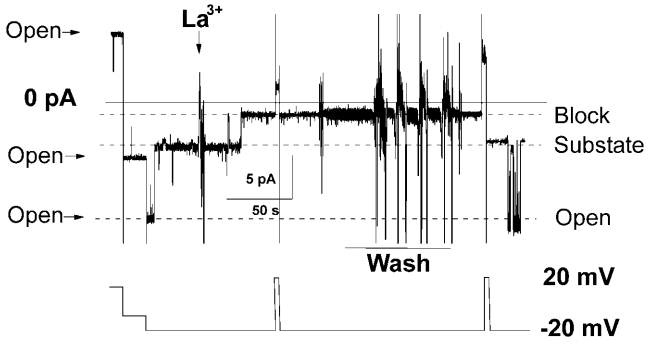

FIGURE 6 Channel block by lanthanum. Added to the *cis* compartment of the bilayer chamber was 0.5 mM of $LaCl_3$. Perfusion to wash out $LaCl_3$ was done by a vacuum pump with simultaneous addition of the lanthanum-free recording solution. Symmetrical recording solutions contained 150 mM KCl, pH = 7.4 (10 mM Hepes-Tris).

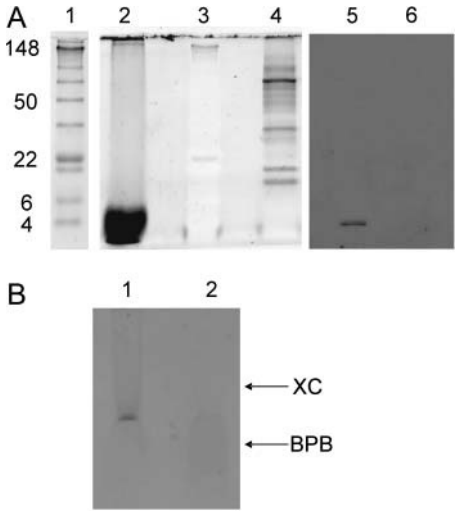

FIGURE 7 Chemical composition of the chloroform extract. (*A*) 10% SDS-PAGE electrophoresis gel stained using the high sensitivity SYPRO Ruby method (*lanes 2–4*) demonstrates drastically reduced protein content of the mitochondrial chloroform extract. (*Lane 1*) Prestained molecular weight standards. (*Lane 2*) Chloroform extract from 100 mg of dehydrated mitochondrial fraction, filtered through 0.2 μm Teflon filter; only low molecular weight peptides are observed. (*Lane 3*) The same standards as in lane 1, visualized by SYPRO Ruby protocol (the prestaining of the standards interferes with the SYPRO Ruby detection). (*Lane 4*) 0.2 mg of dehydrated mitochondrial fraction (500-fold less than in *lane 1*), resuspended in water. Western blots: lane 5 the same sample as in lane 2, and lane 6 the same as lane 4 visualized by antibodies against ATP synthase subunit *c*. (*B*) Toluidine blue staining of chloroform extract in a 15% PAGE gel (see Materials and Methods). (*Lane 1*) Control sample containing chloroform extract treated with protease K (*Lane 2*) The same amount of extract treated with exopolyphosphataseX. The arrows indicate the position of the dye standards on the gel: BPB, bromophenol blue; XC, xylene cyanol.

in the filtered chloroform extract that was used for bilayer experiments. We found no evidence of any protein with molecular weight in the range of ~5–150. This range would be expected to include adenine nucleotide translocator (ANT) and voltage-dependent anionic channel (VDAC), recognized members of the PTP complex (Crompton, 1999). Although chloroform extraction effectively removed proteins in this size range from the preparation, we were able to detect significant amounts of PHB and polyP in the same sample. The presence of PHB in the mitochondrial extract was established by chemical assay (see Materials and Methods). Mitochondrial PHB size, as determined by non-aqueous size-exclusion chromatography, was the same as that of PHB extracted from *E. coli* membranes, previously determined by electrospray mass spectroscopy as 12.2 (Reusch, 2001). The presence of polyP was detected by toluidine blue staining (Fig. 7 *B*, *lane 1*) and its identity was confirmed by degradation with the polyP-specific enzyme, exopolyphosphataseX (Fig. 7 *B*, *lane 2*). The size of the polyP, estimated from its electrophoretic mobility on acrylamide/bis gels (Fig. 7) is 60–70 units, similar to that of polyP from *E. coli* channels (Reusch et al., 1995). The peptide observed in the

chloroform extract was stained by antibodies to subunit C of ATP synthase (Fig. 7 *A*, *lane 5*).

DISCUSSION

We were able to isolate from mitochondria, by extraction with chloroform, an apparently nonproteinaceous complex that can form channels very similar to those seen during the opening of mitochondrial permeability transition pore. Electrophysiological properties of a similar complex, isolated from *E. coli*, have been studied in some detail (Reusch et al., 1995; Das et al., 1997). Although it has been known for a long time that such a complex is present in eukaryotic membranes, including mitochondria (Reusch, 1989), no previous study has investigated its role.

Single-channel properties: comparison with mitoplast studies

In this part of the discussion, we compare the single-channel properties that we observed with the literature data from patch clamp of mitochondrial membranes. Properties of the channel in our experiments are similar to those of the large channel seen in patch-clamp studies of native mitoplasts, which have been identified by Zoratti and co-workers as the mitochondrial megachannel (Szabo and Zoratti, 1991) and by Kinnally and co-workers as the multi-conductance channel (MCC) (Zorov et al., 1992). It was suggested, in both of those cases, that the channel activity corresponded to the opening of the permeability transition pore seen in isolated or native mitochondria; thus in the following discussion we will refer to it as the PTP. It should be noted that properties of the PTP channel have not been well established in part because of its extremely complicated behavior. In Table 1, we summarize known properties of the PTP channel and compare them with our observations on reconstituted channels. We consider the following seven characteristics as typifying the complex behavior of PTP:

TABLE 1 Comparison of the channel properties with PTP (for references see text)

	Chloroform extract	PTP
Maximal conductance (nS)	Up to 0.7	Up to 1.3
Substates	Multiple	Multiple
Voltage dependence	Symmetrical	Nonsymmetrical (but see Discussion for different literature reports)
Selectivity	Variable	Variable
CSA block	No	Yes/no
pH dependence	Irreversibly blocked at pH < 6	Blocked at pH < 6; reversed by calcium
Ca^{2+} activation	No (but see Materials and Methods)	Yes

1. The maximal conductance of the PTP channel in 150 mM KCl is in the range of 1–1.5 nS (Kinnally et al., 1989; Petronilli et al., 1989), although it has been reported that smaller conductance channels with other properties identical to PTP channel can be observed (Loupatatzis et al., 2002). In some experiments, the highest ($\sim$1 nS) conductance state was observed infrequently or not at all (Kinnally et al., 1989), but the authors suggest that the smaller conductance levels represent different states of the same PTP channel (Kinnally et al., 1992). In our experiments, we chose to identify the ''fully open'' channel as the maximal conductance seen in each experiment, using the occurrence of direct transitions from the maximal conductance to near baseline as a criterion for the presence of only one conducting channel. With this criterion, the size of the fully open channel varied from 350 to 750 pS in 150 mM KCl. Thus, the maximal conductance of the reconstituted channel falls in the range of values observed for the PTP channel.
2. The presence of the multiple subconductance states is uniformly reported for the PTP, which has been named the ''multiple conductance channel'', or MCC, for this property (Zorov et al., 1992). This type of the behavior is clearly evident in our experiments.
3. PTP is known to be voltage dependent. It tends to be fully open at the lower voltages and to switch to one of the lower conductance substates with an increase in voltage. There is some contradiction in the literature about this feature of the channel; in some experiments, it was shown that the fully open PTP channel was only rarely observed at voltages higher than $\pm$40 mV (Loupatatzis et al., 2002), whereas in others, it closed only when high matrix-negative voltage was applied (Szabo and Zoratti, 1993). Furthermore, it has been reported that the PTP channel sometimes demonstrates different behavior and stays open at negative voltages but closes at positive voltages (Kinnally et al., 1992). Such differences might arise from the differences in preparations of mitoplasts, which could lead to differences in composition of the PTP forming complex. In our experiments, channel activity was voltage-dependent; the fully open channel at lower voltages tended to switch to lower conductance substates with an increase in applied voltage (Fig. 2 *B*) and this voltage sensitivity was roughly symmetrical around 0 mV. Our observations that the voltage-dependent decrease of conductance in our experiments was symmetrical, whereas in most patch-clamp experiments it occurred only for voltages of one sign, may reflect the fact that in native mitoplasts, the PTP complex remains intact. However, in our reconstitution experiments, a channel-forming structure appears to be isolated from the larger complex. A remarkable parallel exists between our results and observations in yeast mitoplasts. Wild-type yeast MCC channels are

functionally very similar to mammalian PTP, including asymmetric dependence on voltage. However, in VDAC-less yeast mitoplasts, MCC tends to close when the potential is increased regardless of its sign (Lohret and Kinnally, 1995).

4. A fascinating feature of the PTP channel is its variable selectivity. It is known that this channel has different selectivity states that can vary from slightly cationic to slightly anionic (Kinnally et al., 1989; Szabo and Zoratti, 1992). In our experiments, we have found that the channel shows multiple selectivity states and that multiple selectivity transitions can be observed in a single experiment. Mostly, the different selectivity states reflected relatively weak preference for anions or cations, but occasionally we observed periods when channel became strongly selective for potassium over chloride (Fig. 5).
5. Cyclosporin A (CsA) is known to be a potent inhibitor of PTP in mitochondria in vivo and in experiments on isolated mitochondria (for review see (Zoratti and Szabo, 1995)). Hence, this drug has been tested in single channel experiments on mitoplasts. In some reports, the PTP channel was blocked by CsA (Szabo and Zoratti, 1991; Loupatatzis et al., 2002) but in others it was not (Campello et al., 2004). Such apparently contradictory results may be explained by the fact that CsA is known to act by binding to mitochondrial cyclophilin, a protein attached to the PTP complex (Halestrap et al., 1997). It is reasonable to suggest that under some conditions, cyclophilin can dissociate from the PTP complex, resulting in loss of its sensitivity to CsA. We do not find it surprising that the channel in our experiments was insensitive to CsA, because it seems likely that we isolated only the conducting part of the PTP complex, with little or no associated protein, and specifically without the receptor for CsA.
6. Permeability transition in mitochondria can be inhibited by protons, and this inhibition is antagonized by increases in [Ca^{2+}] (Haworth and Hunter, 1979). A similar inhibitory effect, which was reversed by an increase in calcium concentration, has been seen in patch-clamp experiments (Szabo et al., 1992). We have found that a decrease of pH below 6 irreversibly abolishes channel activity (see Results). This irreversibility may result from the fact that, in our bilayer experiments, the channel-forming components may be separated from parts that normally stabilize the PTP complex, allowing the reconstituted channel to be irreversibly destroyed by lower pH. In patch-clamp recordings from native membrane, on the other hand, the PTP complex is likely to be more nearly intact, and the channel is seen to be regulated dynamically by calcium (see following point).
7. PTP can be activated by calcium (Szabo and Zoratti, 1992; Kinnally et al., 1991), whereas in our experiments channel activity was insensitive to calcium addition. However, in three experiments, addition of EGTA (2 mM, with no added calcium in the solutions) destabilized the channel. This may reflect the importance of normal levels of contaminant Ca2+ present in other salts in maintaining a stable polyphosphate complex. This suggestion is supported by our anecdotal observation that channel activity was more reliably achieved when mitochondria were pretreated with calcium-containing solutions before dehydration and chloroform extraction (see Methods). Furthermore, detection frequency of PTP channel in native patch-clamp experiments is dramatically increased when higher levels of calcium are used in the isolation media (Kinnally et al., 1991).

Overall, we conclude that channel activity seen in our experiments compares well to the channel activity of the PTP channel as seen in patch-clamp experiments on mitoplasts.

Channel composition

We adopted an extraction protocol that was previously used to isolate a channel-forming complex of PHB/polyP/Ca^{2+} from *E. coli*. Applied to mitochondria, this protocol allowed us to reconstitute channel activity resembling the mitochondrial PTP. A central issue now is to identify the components of the chloroform extract underlying the channel activity.

First, taking into account that this channel activity is similar to PTP, we should consider that it might be due to the presence of the channel-forming proteins, which have been identified as parts of PTP. These include VDAC or ANT. We think it very unlikely that these proteins were present in the reconstituted channels in our experiments. Previous work on hydrophobic extraction of mitochondrial membrane component did not reveal proteins such as VDAC or ANT in the extract (Mironova et al., 1997; Azarashvily et al., 2000). These earlier experiments used chloroform-methanol mixtures as extraction media, whereas in our experiments we used pure chloroform for extraction. This is even more hydrophobic, suggesting an even smaller likelihood that proteins like VDAC or ANT would be extracted. In agreement with literature data, we were not able to detect presence of any protein with a molecular weight in the range of ~5–150 in our extract (Fig. 7).

We estimate that, to obtain 50% probability of a protein channel incorporation into a bilayer with a diameter of 100 μm, at least 1 pg of active channel-forming protein should be present per 1 mg of lipid (assuming that a minimal weight of one functional protein molecule is 35 and one lipid molecule weighs 800 and occupies 75 $Å^2$ of membrane surface). This estimate gives a rough theoretical limit for the minimal amount of active protein, which would be needed to give reasonable probability of channel incorporation. In fact, the amount of total protein may need to be significantly higher

because it is likely that only part of the protein would be folded properly to form a functional channel. In our SYPRO Ruby stained gels (Fig. 7), 1000 times more extracted material was applied to the gel than was used for each bilayer reconstitution experiment. This implies that protein equivalent to the presence of picogram amounts in bilayer experiment should have been revealed by SYPRO Ruby staining, if previously reported channel-forming proteins were contributing to our observed activity (detection limit <10 ng). The lack of bands, from the chloroform-extracted material, of a molecular weight appropriate for VDAC or ANT makes it unlikely that these contribute to our recordings.

A second possibility is that observed channel activity might be due to the presence in the hydrophobic extract of a low-molecular component, other than PHB/polyP/Ca^{2+}. Indeed, the chloroform extract used in our experiments contained low-molecular weight peptide, which gave a positive reaction to antibodies against the ATPase subunit C (Fig. 7). Under certain conditions, subunit C, or a similar peptide, can form channels, but with the properties very different from those seen in our experiments (McGeoch and Guidotti, 1997). Furthermore, this channel can be blocked by subunit C antibodies, which was not seen in our experiments. Another possibility is involvement of free fatty acids in the channel formation. Free fatty acids were shown to be present in a hydrophobic mitochondrial extract and are able to induce nonspecific conductance in the artificial bilayers (Mironova et al., 2001). However, these have been shown to cause nonspecific leak conductance, rather than stable channel activity, and require presence of high (5 mM) concentrations of calcium for this action.

Overall, we conclude that neither these low-molecular weight nonpeptide components, nor any known mitochondrial channel-forming proteins, were necessary and sufficient for the channel activity seen in our experiments. This conclusion is further supported by the fact that dehydration of the mitochondrial preparation by acetone before chloroform extraction was an absolute requirement for channel activity in our experiments, whereas the presence of water would still allow effective extraction of fatty acids and/or subunit C peptide.

After critical consideration of these other possibilities, we suggest that the channel activity seen in our experiments is most likely to result from the presence of a PHB/polyP/Ca^{2+} complex in the hydrophobic extract. Dehydration of the membrane fraction before extraction is a requirement for isolation of intact PHB/polyP/Ca^{2+} channels. Significant amounts of PHB and polyphosphate were detected in our chloroform extracts (see Results). Presence of highly polar polyphosphate in the relatively hydrophobic chloroform extract indicates that it is extracted in a form of a complex (presumably with PHB and calcium). Unexpectedly, the channel activity in our experiments differed significantly from the channel activity reported for a synthetic PHB/polyP/Ca^{2+} complex (Das et al., 1997) and for a PHB/polyP/Ca^{2+} complex isolated from *E. coli* (Reusch et al., 1995). Specifically, this complex has not been observed to form large voltage-dependent, weakly selective channels at the lower voltages. Nonetheless, channel behavior at higher voltages in our experiments was strikingly similar to the behavior of the PHB/polyP/Ca^{2+} channel. This included channel size (Das et al., 1997), gating modes (Das and Reusch, 1999), cationic selectivity (Das and Reusch, 2001), and sensitivity to the lanthanum (Das et al., 1997).

A model, proposed for the conformation of the PHB/polyP/Ca^{2+} channel complex, suggests that this complex is formed by a membrane-spanning cylinder of PHB molecules with polyP located inside the PHB shell (Das et al., 1997). However, it has also been shown that PHB alone can form channels in lipid bilayers (Seebach et al., 1996). It seems reasonable to us that a channel formed, in whole or in part, from the building blocks of PHB, polyp, and Ca^{2+}, with the possibility of different levels of oligomerization, might be a dynamic structure showing multiple conformations, depending on chemical conditions, transmembrane electric field, and/or the presence or absence of accessory molecules. It does not seem surprising that these channels might exhibit the complexity of behavior that we and others have observed, including multiple subconductances, and discretely variable selectivity. We do not, however, think it is worthwhile to attempt to provide detailed a priori explanations of this complex behavior at this time. Lessons from recent studies of protein channels show the difficulties of prediction of mechanism of conduction mechanism even with a full sequence, and much functional data and homology analysis in hand. For example, the role of the backbone carbonyl oxygen atoms in K channel selectivity was not clear until a high resolution structure of the channel became available (Doyle et al., 1998). Similarly, the bacterial sodium channel, NaChBac, was proposed to be a calcium channel until it was expressed and studied experimentally (Durell and Guy, 2001; Ren et al., 2001). Nonetheless, a PHB/polyP/Ca^{2+} complex certainly seems to offer sufficient degrees of structural freedom—for example, by redistribution of polyP and Ca^{2+} within the structure in response to voltage changes—to provide a plausible basis for the many complexities of behavior that we observe.

Differences in detail between the channel properties that we have observed, and records from mitoplasts, bacterial systems, or completely synthetic channels, may reflect slightly different complexes built from the same set of building blocks, in different proportions and conformations. There is a possibility that a PHB/polyP/Ca^{2+} complex from mitochondria may be assembled, or may incorporate accessory subunits, in a way that makes it unique to mitochondria, and that this may underlie some unique aspects of channel behavior seen in our experiments. However, the multi-faceted parallels, shown by recordings from these different preparations, argue strongly for common structural elements underlying the behavior.

Possible involvement of the PHB/polyP/Ca^{2+} complex in formation of the mitochondrial permeability transition pore

The regulation of the PTP activity is known to be very complicated (for a review, see Zoratti and Szabo, 1995), and the nature of the conductance pathway of the PTP remains unclear. It is generally believed that PTP is formed by a protein complex, which includes ANT as a channel-forming component, located at the inner mitochondrial membrane (Halestrap and Brennerb, 2003). This conclusion is based on the fact that PTP activity can be regulated by ligands of ANT (Halestrap and Brennerb, 2003) and that purified, recombinant ANT protein can form PTP-like channels when reconstituted into bilayers (Brustovetsky et al., 2002). Subsequently, experiments by Kokoszka and collaborators, using mitochondria from ANT-knockout mice, suggested that ANT is not essential for PTP formation, but rather plays a regulatory role (Kokoszka et al., 2004), though expression of additional ANT-like genes may complicate the interpretation of these experiments (Halestrap, 2004). In parallel with the results of Kokoszka et al., our experiments show that PTP-like channel activity can be observed in a preparation that does not contain any detectable amount of ANT. In ANT-knockout mitochondria, PTP opening could still be induced by a decrease of the potential difference across the inner mitochondrial membrane. Similarly, channel activation at reduced voltages was seen in our bilayer experiments (Fig. 2).

We suggest that we were able to isolate the ion-conducting part of the mitochondrial PTP complex. Most likely, in live mitochondria, this complex is tightly linked to protein components of the PTP complex, similar to cases for complexes of PHB/polyP/Ca^{2+} with cytoplasmic and membrane proteins (Huang and Reusch, 1996), including ion channel proteins (Zakharian and Reusch, 2004). The fact that in our experiments PHB/polyP/Ca^{2+} can be separated from the proteins by chloroform extraction indicates that, in our case, binding between the complex and proteins is noncovalent. It is important to note that experiments on isolated mitochondria suggest the existence of high-conductance, weakly cation-selective, and low-conductance, cation-selective conformations of the mitochondrial permeability transition pore (Ichas and Mazat, 1998). Properties of the channel seen in our experiments indicate that, at higher voltages, it can be small and cation-selective, opening the possibility that the PHB/polyP/Ca^{2+} complex might be responsible for both high- and low-conductance pores depending on conditions.

CONCLUSION

By applying an anhydrous chloroform extraction method to mitochondrial membranes, we were able to isolate channels, with a reproducible but strikingly unusual and complex combination of properties; these properties mimic the behavior of the mitochondrial permeability transition pore. Our data are consistent with the hypothesis that this channel represents at least a part of the structure of the mitochondrial permeability transition pore.

This work was supported by operating grants from the Canadian Institutes of Health Research, the National Institutes of Health (GM054090), and the National Science Foundation (0422938). R.J.F. is a Heritage Medical Scientist of the Alberta Heritage Foundation for Medical Research.

We thank Drs. J. Coorssen and Roby Butt for assistance with SYPRO Ruby assay, and Drs. Paul Schnetkamp and Gerald Zamponi for critical comments on a draft of the manuscript. We are grateful to Dr. D. N. Palmer, Lincoln University, New Zealand, for providing subunit C antibodies, and Dr. A. Kornberg, Stanford University, Stanford, CA, for providing exopolyphosphataseX.

REFERENCES

Accardi, A., and C. Miller. 2004. Secondary active transport mediated by a prokaryotic homologue of ClC Cl^- channels. *Nature*. 427:803–807.

Azarashvily, T. S., J. Tyynela, M. Baumann, Y. V. Evtodienko, and N. E. Saris. 2000. Ca^{2+}-modulated phosphorylation of a low-molecular-mass polypeptide in rat liver mitochondria: evidence that it is identical with subunit c of F(0)F(1)-ATPase. *Biochem. Biophys. Res. Commun.* 270: 741–744.

Barry, P. H. 1994. JPCalc, a software package for calculating liquid junction potential corrections in patch-clamp, intracellular, epithelial and bilayer measurements and for correcting junction potential measurements. *J. Neurosci. Methods*. 51:107–116.

Brookes, P. S., Y. Yoon, J. L. Robotham, M. W. Anders, and S. S. Sheu. 2004. Calcium, ATP, and ROS: a mitochondrial love-hate triangle. *Am. J. Physiol. Cell Physiol.* 287:C817–C833.

Brustovetsky, N., M. Tropschug, S. Heimpel, D. Heidkamper, and M. Klingenberg. 2002. A large Ca^{2+}-dependent channel formed by recombinant ADP/ATP carrier from Neurospora crassa resembles the mitochondrial permeability transition pore. *Biochemistry*. 41:11804–11811.

Campello, S., U. De Marchi, I. Szabo, F. Tombola, and M. Zoratti. 2004. Bax is not relevant for the Ca-induced Mitochondrial Permeability Transition. *Biophys. J.* 86:461a. (Abstr.)

Carafoli, E. 2003. Historical review: mitochondria and calcium: ups and downs of an unusual relationship. *Trends Biochem. Sci.* 28:175–181.

Crompton, M. 1999. The mitochondrial permeability transition pore and its role in cell death. *Biochem. J.* 341:233–249.

Danial, N. N., and S. J. Korsmeyer. 2004. Cell death: critical control points. *Cell.* 116:205–219.

Das, S., U. D. Lengweiler, D. Seebach, and R. N. Reusch. 1997. Proof for a nonproteinaceous calcium-selective channel in *Escherichia coli* by total synthesis from (R)-3-hydroxybutanoic acid and inorganic polyphosphate. *Proc. Natl. Acad. Sci. USA*. 94:9075–9079.

Das, S., and R. N. Reusch. 1999. Gating kinetics of *E. coli* poly-3-hydroxybutyrate/polyphosphate channels in planar bilayer membranes. *J. Membr. Biol.* 170:135–145.

Das, S., and R. N. Reusch. 2001. pH regulates cation selectivity of poly-(R)-3-hydroxybutyrate/polyphosphate channels from *E. coli* in planar lipid bilayers. *Biochemistry*. 40:2075–2079.

Das, S., D. Seebach, and R. N. Reusch. 2002. Differential effects of temperature on *E. coli* and synthetic polyhydroxybutyrate/polyphosphate channels. *Biochemistry*. 41:5307–5312.

Doyle, D. A., C. J. Morais, R. A. Pfuetzner, A. Kuo, J. M. Gulbis, S. L. Cohen, B. T. Chait, and R. MacKinnon. 1998. The structure of the potassium channel: molecular basis of K^+ conduction and selectivity. *Science*. 280:69–77.

Durell, S. R., and H. R. Guy. 2001. A putative prokaryote voltage-gated Ca^{2+} channel with only one 6TM motif per subunit. *Biochem. Biophys. Res. Commun.* 281:741–746.

Dyall, S. D., M. T. Brown, and P. J. Johnson. 2004. Ancient invasions: from endosymbionts to organelles. *Science.* 304:253–257.

Garlid, K. D., and P. Paucek. 2001. The mitochondrial potassium cycle. *IUBMB Life.* 52:153–158.

Green, D. R., and G. Kroemer. 2004. The pathophysiology of mitochondrial cell death. *Science.* 305:626–629.

Halestrap, A. P. 2004. Mitochondrial permeability: dual role for the ADP/ATP translocator? *Nature.* 430:1.

Halestrap, A. P., and C. Brennerb. 2003. The adenine nucleotide translocase: a central component of the mitochondrial permeability transition pore and key player in cell death. *Curr. Med. Chem.* 10:1507–1525.

Halestrap, A. P., C. P. Connern, E. J. Griffiths, and P. M. Kerr. 1997. Cyclosporin A binding to mitochondrial cyclophilin inhibits the permeability transition pore and protects hearts from ischaemia/reperfusion injury. *Mol. Cell. Biochem.* 174:167–172.

Haworth, R. A., and D. R. Hunter. 1979. The Ca^{2+}-induced membrane transition in mitochondria. II. Nature of the Ca2+ trigger site. *Arch. Biochem. Biophys.* 195:460–467.

Huang, R., and R. N. Reusch. 1996. Poly(3-hydroxybutyrate) is associated with specific proteins in the cytoplasm and membranes of *Escherichia coli*. *J. Biol. Chem.* 271:22196–22202.

Ichas, F., and J. P. Mazat. 1998. From calcium signaling to cell death: two conformations for the mitochondrial permeability transition pore. Switching from low- to high-conductance state. *Biochim. Biophys. Acta.* 1366:33–50.

Karr, D. B., J. K. Waters, and D. W. Emerich. 1983. Analysis of poly-β-hydroxybutyrate in Rhizobium japonicum bacteroids by ion-exclusion high-pressure liquid chromatography and UV detection. *Appl. Environ. Microbiol.* 46:1339–1344.

Kinnally, K. W., Y. N. Antonenko, and D. B. Zorov. 1992. Modulation of inner mitochondrial membrane channel activity. *J. Bioenerg. Biomembr.* 24:99–110.

Kinnally, K. W., M. L. Campo, and H. Tedeschi. 1989. Mitochondrial channel activity studied by patch-clamping mitoplasts. *J. Bioenerg. Biomembr.* 21:497–506.

Kinnally, K. W., D. Zorov, Y. Antonenko, and S. Perini. 1991. Calcium modulation of mitochondrial inner membrane channel activity. *Biochem. Biophys. Res. Commun.* 176:1183–1188.

Kokoszka, J. E., K. G. Waymire, S. E. Levy, J. E. Sligh, J. Cai, D. P. Jones, G. R. MacGregor, and D. C. Wallace. 2004. The ADP/ATP translocator is not essential for the mitochondrial permeability transition pore. *Nature.* 427:461–465.

Lohret, T. A., and K. W. Kinnally. 1995. Multiple conductance channel activity of wild-type and voltage-dependent anion-selective channel (VDAC)-less yeast mitochondria. *Biophys. J.* 68:2299–2309.

Loupatatzis, C., G. Seitz, P. Schonfeld, F. Lang, and D. Siemen. 2002. Single-channel currents of the permeability transition pore from the inner mitochondrial membrane of rat liver and of a human hepatoma cell line. *Cell. Physiol. Biochem.* 12:269–278.

Mattson, M. P., and G. Kroemer. 2003. Mitochondria in cell death: novel targets for neuroprotection and cardioprotection. *Trends Mol. Med.* 9: 196–205.

McGeoch, J. E., and G. Guidotti. 1997. A 0.1–700 Hz current through a voltage-clamped pore: candidate protein for initiator of neural oscillations. *Brain Res.* 766:188–194.

Mironova, G. D., O. Gateau-Roesch, C. Levrat, E. Gritsenko, E. Pavlov, A. V. Lazareva, E. Limarenko, C. Rey, P. Louisot, and N. E. Saris. 2001. Palmitic and stearic acids bind Ca^{2+} with high affinity and form nonspecific channels in black-lipid membranes. Possible relation to Ca^{2+}-activated mitochondrial pores. *J. Bioenerg. Biomembr.* 33:319–331.

Mironova, G. D., A. Lazareva, O. Gateau-Roesch, J. Tyynela, Y. Pavlov, M. Vanier, and N. E. Saris. 1997. Oscillating Ca^{2+}-induced channel activity obtained in BLM with a mitochondrial membrane component. *J. Bioenerg. Biomembr.* 29:561–569.

Palmer, D. N., S. L. Bayliss, and V. J. Westlake. 1995. Batten disease and the ATP synthase subunit c turnover pathway: raising antibodies to subunit c. *Am. J. Med. Genet.* 57:260–265.

Petronilli, V., I. Szabo, and M. Zoratti. 1989. The inner mitochondrial membrane contains ion-conducting channels similar to those found in bacteria. *FEBS Lett.* 259:137–143.

Ren, D., B. Navarro, H. Xu, L. Yue, Q. Shi, and D. E. Clapham. 2001. A prokaryotic voltage-gated sodium channel. *Science.* 294:2372–2375.

Reusch, R. N. 1989. Poly-beta-hydroxybutyrate/calcium polyphosphate complexes in eukaryotic membranes. *Proc. Soc. Exp. Biol. Med.* 191: 377–381.

Reusch, R. N. 2001. Nonstorage polyhydroxyalkanoates (complexed PHAs) in prokaryotes and eukaryotes. *In* Biopolymers, Vol. 3A. Y. Doi and A. Steinbuchel, editors. Wiley VCH, Weinheim, Germany. 123–172.

Reusch, R. N., R. Huang, and L. L. Bramble. 1995. Poly-3-hydroxybutyrate/polyphosphate complexes form voltage-activated Ca^{2+} channels in the plasma membranes of *Escherichia coli*. *Biophys. J.* 69:754–766.

Seebach, D., A. Brunner, H. M. Burger, R. N. Reusch, and L. L. Bramble. 1996. Channel-forming activity of 3-hydroxybutanoic-acid oligomers in planar lipid bilayers. *Helv. Chim. Acta.* 79:507–517.

Szabo, I., P. Bernardi, and M. Zoratti. 1992. Modulation of the mitochondrial megachannel by divalent cations and protons. *J. Biol. Chem.* 267:2940–2946.

Szabo, I., and M. Zoratti. 1991. The giant channel of the inner mitochondrial membrane is inhibited by cyclosporin A. *J. Biol. Chem.* 266: 3376–3379.

Szabo, I., and M. Zoratti. 1992. The mitochondrial megachannel is the permeability transition pore. *J. Bioenerg. Biomembr.* 24:111–117.

Szabo, I., and M. Zoratti. 1993. The mitochondrial permeability transition pore may comprise VDAC molecules. I. Binary structure and voltage dependence of the pore. *FEBS Lett.* 330:201–205.

Wurst, H., and A. Kornberg. 1994. A soluble exopolyphosphatase of *Saccharomyces cerevisiae*. Purification and characterization. *J. Biol. Chem.* 269:10996–11001.

Zakharian, E., and R. N. Reusch. 2004. Functional evidence for a supramolecular structure for the *Streptomyces lividans* potassium channel KcsA. *Biochem. Biophys. Res. Commun.* 322:1059–1065.

Zoratti, M., and I. Szabo. 1995. The mitochondrial permeability transition. *Biochim. Biophys. Acta.* 1241:139–176.

Zorov, D. B., K. W. Kinnally, S. Perini, and H. Tedeschi. 1992. Multiple conductance levels in rat heart inner mitochondrial membranes studied by patch clamping. *Biochim. Biophys. Acta.* 1105:263–270.